

# Cysteamine Modulates Oxidative Stress and Blocks Myofibroblast Activity in CKD

Daryl M. Okamura,\* Nadia M. Bahrami,\* Shuyu Ren,<sup>†</sup> Katie Pasichnyk,\* Juliana M. Williams,\* Jon A. Gangoiti,<sup>‡</sup> Jesus M. Lopez-Guisa,\* Ikuyo Yamaguchi,\* Bruce A. Barshop,<sup>‡</sup> Jeremy S. Duffield,<sup>†</sup> and Allison A. Eddy\*

\*Seattle Children's Hospital Research Institute, University of Washington, Seattle, Washington; <sup>†</sup>Division of Nephrology, Center for Lung Biology, Department of Medicine, and Institute of Stem Cell and Regenerative Medicine, University of Washington, Seattle, Washington; and <sup>‡</sup>Department of Pediatrics, University of California, San Diego, La Jolla, California

## ABSTRACT

Therapy to slow the relentless expansion of interstitial extracellular matrix that leads to renal functional decline in patients with CKD is currently lacking. Because chronic kidney injury increases tissue oxidative stress, we evaluated the antifibrotic efficacy of cysteamine bitartrate, an antioxidant therapy for patients with nephropathic cystinosis, in a mouse model of unilateral ureteral obstruction. Fresh cysteamine (600 mg/kg) was added to drinking water daily beginning on the day of surgery, and outcomes were assessed on days 7, 14, and 21 after surgery. Plasma cysteamine levels showed diurnal variation, with peak levels similar to those observed in patients with cystinosis. In cysteamine-treated mice, fibrosis severity decreased significantly at 14 and 21 days after unilateral ureteral obstruction, and renal oxidized protein levels decreased at each time point, suggesting reduced oxidative stress. Consistent with these results, treatment of cultured macrophages with cysteamine reduced cellular generation of reactive oxygen species. Furthermore, treatment with cysteamine reduced  $\alpha$ -smooth muscle actin–positive interstitial myofibroblast proliferation and mRNA levels of extracellular matrix proteins in mice and attenuated myofibroblast differentiation and proliferation *in vitro*, but did not augment TGF- $\beta$  signaling. In a study of renal ischemia reperfusion, cysteamine therapy initiated 10 days after injury and continued for 14 days decreased renal fibrosis by 40%. Taken together, these data suggest previously unrecognized antifibrotic actions of cysteamine *via* TGF- $\beta$ –independent mechanisms that include oxidative stress reduction and attenuation of the myofibroblast response to kidney injury and support further investigation into the potential benefit of cysteamine therapy in the treatment of CKD.

*J Am Soc Nephrol* 25: ●●–●●, 2013. doi: 10.1681/ASN.2012090962

Oxidative stress reflects a perturbation in redox potential due to an imbalance between the rates of oxidant generation and the availability of antioxidants. Several studies indicate that the consequences of this redox imbalance are not simply a random process, but a highly regulated one that targets specific amino acids or lipid moieties in a pathway- and

cell type–specific manner.<sup>1–3</sup> For example, a recent study demonstrated that oxidized phospholipids are essential mediators of TNF- $\alpha$  receptor signaling response to mitochondrial damage and cell death.<sup>4</sup> Thiol proteins serve as one of the primary antioxidant defense systems, both intracellular and extracellular. Thiol groups react with almost all

physiologic oxidants and can reduce them before they trigger harmful reactions.<sup>5</sup> Chronic kidney injury depletes endogenous intracellular and extracellular antioxidant systems, resulting in increased tissue oxidative stress.<sup>6–8</sup>

Cysteamine bitartrate is a simple yet interesting aminothiols that is approved by the US Food and Drug Administration for the treatment of patients with cystinosis. Before the availability of cysteamine, most patients with nephropathic cystinosis developed ESRD within the first decade of life.<sup>9,10</sup> Its efficacy as a renoprotective agent in nephropathic cystinosis is well established, yet the specific protective mechanisms remain incompletely understood. There is no question that cysteamine dramatically lowers intracellular levels of cytotoxic cystine, but this effect alone does not fully explain its renoprotective effects and led us to consider an alternative mechanism of action. Recent studies suggest that cysteamine

Received September 29, 2012. Accepted June 19, 2013.

Published online ahead of print. Publication date available at www.jasn.org.

**Correspondence:** Dr. Daryl M. Okamura, Seattle Children's Research Institute, Center for Developmental Biology and Regenerative Medicine, 1900 Ninth Avenue, CS9-5, Seattle, WA 98101. Email: daryl.okamura@seattlechildrens.org

Copyright © 2013 by the American Society of Nephrology

may have several other potential therapeutic applications beyond cystinosis, such as neurodegenerative disease,<sup>11</sup> cancer,<sup>12</sup> and nonalcoholic liver disease.<sup>13,14</sup>

In this study, we investigated the effects of cysteamine bitartrate therapy in two mouse models of CKD unrelated to cystinosis. The findings provide evidence that cysteamine bitartrate has significant fibrosis-attenuating properties and implicate reduced oxidative stress and attenuated myofibroblast responses as mechanisms.

**RESULTS**

**Cysteamine Is Antifibrotic during Chronic Kidney Injury**

*Cysteamine Pharmacokinetics*  
 Pilot studies for dose efficacy determined that 600 mg/kg of cysteamine administered in the drinking water was the most effective antifibrotic dose (Supplemental Figure 1). In order to make relevant comparisons to human dosing data and to consider the possibility of time-of-day variations pertaining to rodent nocturnal drinking patterns, serial serum cysteamine levels were measured by mass spectrometry in normal mice. After a 2-day run-in period on cysteamine, levels in the range considered therapeutic in patients with cystinosis were only achieved at night. The highest concentrations ( $C_{max}$ ) were between 15 and 20  $\mu\text{mol/L}$  ( $n=4$  per group, Figure 1), which is similar to levels reported in humans.<sup>15</sup>

*Fibrosis Severity Attenuation with Cysteamine*

To investigate the antifibrotic potential of cysteamine after unilateral ureteral obstruction (UO), total collagen levels were measured as the hydroxyproline content per wet kidney weight. Kidney collagen levels were significantly reduced by 21% and 25% in cysteamine-treated mice compared with controls at days 14 and 21 after UO, respectively ( $n=8-10$  per group,  $P<0.01$ , Figure 2A). Computer-assisted semiquantitative image analysis of picrosirius red-stained kidney tissue sections provided histologic confirmation that interstitial collagen expansion was significantly reduced (by

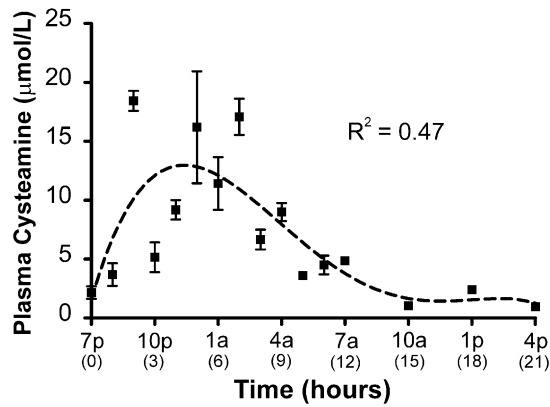


**Figure 1.** Plasma cysteamine levels. Mice are given free access to drinking water containing cysteamine, calculated to deliver a cysteamine dose of 600 mg/kg, for a run-in period of 3 days, after which plasma levels are serially measured in mice hourly between 7 PM and 7 AM, and every 3 hours from 7 AM to 7 PM ( $n=4$  per group). A nonlinear fit of data is performed on the entire data set starting from 7 PM. Results are shown as the mean  $\pm$  1 SEM.

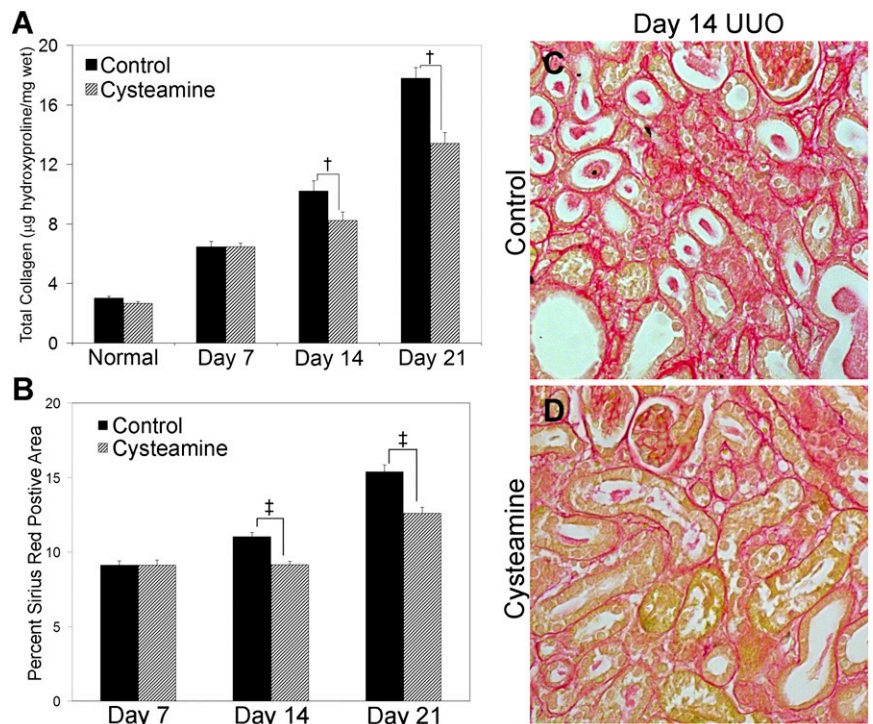


**Figure 2.** Fibrosis severity is attenuated in cysteamine-treated mice. (A) Total kidney collagen content, measured using the hydroxyproline assay, is significantly decreased in the obstructed kidneys of the cysteamine-treated mice (hatched bars) compared with controls (solid bars) on days 14 and 21 ( $n=8$  mice per group). (B) The graph summarizes the results of picrosirius red-positive interstitial collagen quantification, with representative light photomicrographs (C and D) that confirmed diminished matrix deposition at days 14 and 21 in cysteamine-treated mice ( $n=6$  per group). Results are expressed as the mean  $\pm$  SEM.  $^{\dagger}P<0.01$ ;  $^{\ddagger}P<0.05$ , control versus cysteamine-treated groups. Original magnification,  $\times 400$  in C and D.

approximately 18%) in cysteamine-treated mice compared with controls at days 14 and 21 after UO ( $n=8$  per group,  $P<0.01$ , Figure 2, B–D).

*Oxidative Stress Reduction by Cysteamine*

Intracellular redox reactions of thiol proteins are considered a major antioxidant

mechanism. Because cysteamine can act as a biologic thiol, we considered the possibility that cysteamine-based thiol reactions might reduce oxidative stress and kidney injury. The total thiol content was measured in UUO kidneys of control and cysteamine-treated mice and was found to be significantly increased by 53% on day 7 in cysteamine-treated mice compared with the control group; the levels achieved approximated those observed in the contralateral kidney. However, there was no difference observed on days 14 and 21 after UUO (Figure 3A).

Although the specific molecular mechanisms of oxidant stress–induced chronic kidney injury are multiple and incompletely understood, proteins are vulnerable targets. Therefore, kidney carbonylated protein levels were measured as a generalized marker of the protein oxidation status. Free radical interactions with certain amino acid residues (particularly histidine,

arginine, lysine, and proline) produce products expressing carbonyl groups. Carbonyl protein levels were significantly decreased by 34% and 65% in cysteamine-treated mice on days 7 and 14, respectively; a nonsignificant decrease of 48% was present on day 21 (Figure 3B).

#### Cysteamine Does Not Affect Kidney Transglutaminase Activity

In addition to its role as an antioxidant, cysteamine is also known to inhibit the enzyme tissue transglutaminase 2 (Tgm2). Reduced Tgm2 activity has been implicated as a mechanism of cysteamine neuroprotection in experimental mouse models.<sup>11</sup> Increased Tgm2 activity has been reported in humans with CKD as well as in animal models of CKD, and has been associated with enhanced matrix accumulation and fibrosis due to its ability to cross-link proteins within extracellular matrix (ECM),

making them more resistant to proteolytic degradation.<sup>16–18</sup> Therefore, we measured the effects of cysteamine therapy on kidney Tgm2 activity levels in tissue homogenates. Tgm2 activity levels on days 7, 14, and 21 after UUO in cysteamine-treated mice were similar to controls (Figure 4), suggesting that the protective effect of cysteamine is independent of Tgm2.

To further investigate the potential renoprotective mechanisms of cysteamine, additional studies focused on the induction phase of fibrogenesis *in vivo* using the UUO model (days 7 and 14) and *in vitro* using TGF- $\beta$ –treated normal rat kidney interstitial fibroblasts (NRK-49F).

#### Cysteamine Attenuates Macrophage Accumulation but Not Their Microenvironment

Because macrophages are important modulators of oxidant stress and chronic kidney injury, we questioned whether cysteamine therapy might modify their recruitment and/or functional polarity in response to chronic injury. The number of F4/80+ interstitial macrophages was similar between the cysteamine-treated and vehicle-treated mice on day 7, but significantly fewer macrophages were present by day 14 (Figure 5). Whether this late effect is directly mediated by cysteamine or is a secondary consequence of reduced injury is not yet clear. On the basis of cytokine and oxidant mRNA profiling (TNF- $\alpha$ , TNF- $\alpha$  receptor, IL-1 $\beta$ , IL-1 $\beta$  receptor, and NADPH oxidases 2 and 4 [Nox2 and Nox4]) (Supplemental Table 1), cysteamine therapy did not significantly alter their microenvironment.

#### Cysteamine Modulates Reactive Oxygen Species Generation

Previous studies from our laboratory demonstrated that macrophages are a significant source of oxidant generation.<sup>19,20</sup> We hypothesized that cysteamine might modulate reactive oxygen species (ROS) generation in macrophages, leading to an overall reduction in oxidative stress at advanced stages of tissue injury. We examined the effect of cysteamine on

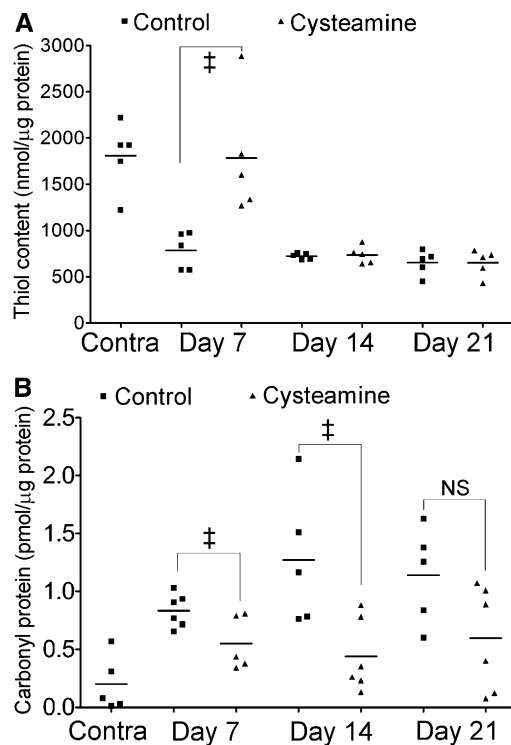


**Figure 3.** Oxidative stress is reduced with cysteamine treatment. Tissue from UUO and contralateral (contra) kidneys is homogenized in cold modified radioimmunoprecipitation assay buffer with inhibitors of thiol oxidation. Total kidney thiols (A) and carbonyl proteins (B) are measured and normalized to total protein. Black squares represent control mice and black triangles represent cysteamine-treated mice. Results are expressed as the mean ± SEM. † $P < 0.05$ , control versus cysteamine-treated groups. NS, not significant.

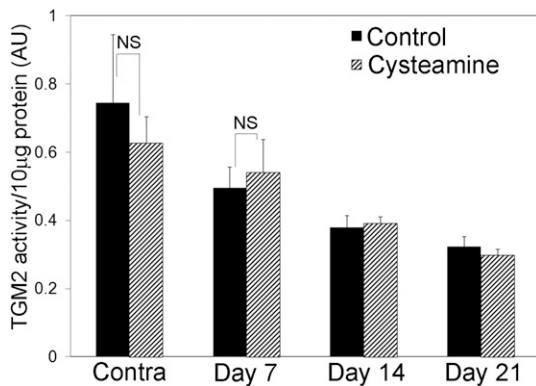


**Figure 4.** Kidney transglutaminase activity is unaltered by cysteamine therapy. Transglutaminase activity, measured in total kidney homogenates, does not show any significant differences ( $n=6$  per group). Solid bars represent control mice and hatched bars represent cysteamine-treated mice. Results are expressed as the mean  $\pm$  SEM. Contra, contralateral unobstructed kidney; NS, not significant.

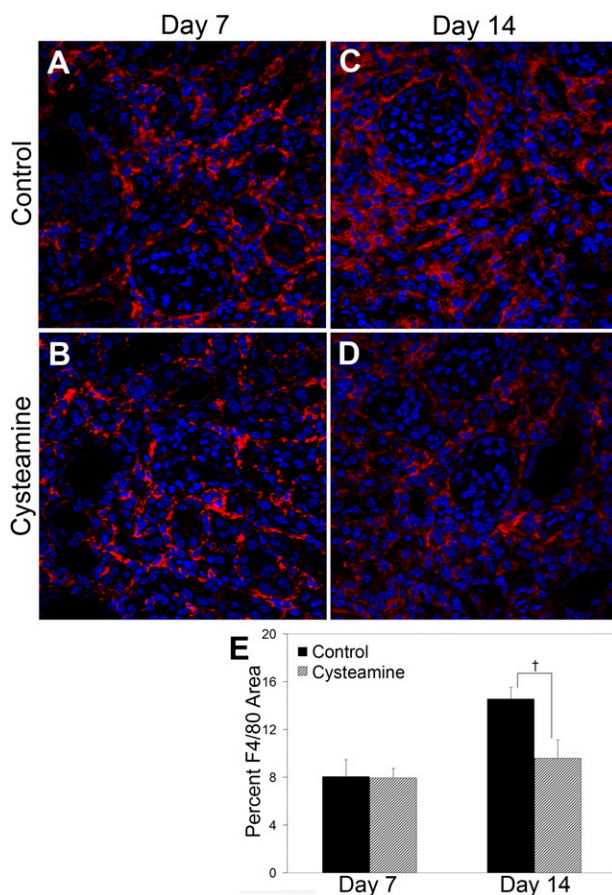


**Figure 5.** Macrophage infiltration is diminished in cysteamine-treated mice. (A–D) Representative confocal images illustrate F4/80-stained interstitial cells. (E) The graph summarizes the semiquantitative results of F4/80+ interstitial staining ( $n=8$  per group). F4/80 (red), nuclei (blue). Results are expressed as the mean  $\pm$  SEM.  $^{\dagger}P<0.01$ , control versus cysteamine-treated groups. NS, not significant. Original magnification,  $\times 400$ .

extracellular ROS generation in PMA-stimulated RAW macrophages using the well established chemiluminescence assay.<sup>21,22</sup> Cysteamine reduced ROS generation by 33% in PMA-stimulated macrophages (Figure 6A). Because the phagocytosis of apoptotic cells is an important inherent function of macrophages, we measured intracellular oxidant generation in macrophages cocultured with apoptotic renal tubular cells. We found that the levels of intracellular oxidant species generated in response to apoptotic cell phagocytosis were reduced by 43%–52% in cysteamine-treated macrophages (Figure 6, B–D). This reduction in oxidant species was seen despite a nearly 2-fold increase in phagocytosis efficiency with cysteamine treatment (control versus cysteamine:  $25.5 \pm 0.7$  versus  $49.5 \pm 2.4$ ,  $n=3$  per group,  $P=0.0003$ ).

### Cysteamine Blocks Myofibroblast Proliferation and Activation

#### Myofibroblast Accumulation

Differentiated myofibroblasts (identified as  $\alpha$ -smooth muscle actin [ $\alpha$ SMA+] cells) are the primary cells that produce ECM during kidney fibrogenesis. Cysteamine therapy significantly reduced the number of  $\alpha$ SMA+ interstitial cells by 47% and 33% at days 7 and 14, respectively, compared with controls (Figure 7, A–C). To determine whether these differences had functional consequences on matrix synthesis rates, kidney mRNA levels were measured for the ECM protein fibronectin and the fibrillar collagens procollagen I and III. The greatest difference in ECM transcription was observed on day 7, when fibronectin, procollagen I, and procollagen III mRNA were reduced by  $>50\%$  in the cysteamine-treated mice compared with controls. On day 14, procollagen I mRNA levels remained significantly suppressed but the lower fibronectin mRNA did not reach statistical significance ( $P=0.08$ ) (Figure 7, D–F).

Given the central role of the TGF- $\beta$ –Smad3 cytokine signaling pathway in myofibroblast activation and fibrogenesis, kidney phospho-Smad3 protein levels were measured in total kidney homogenates by Western blotting. The levels

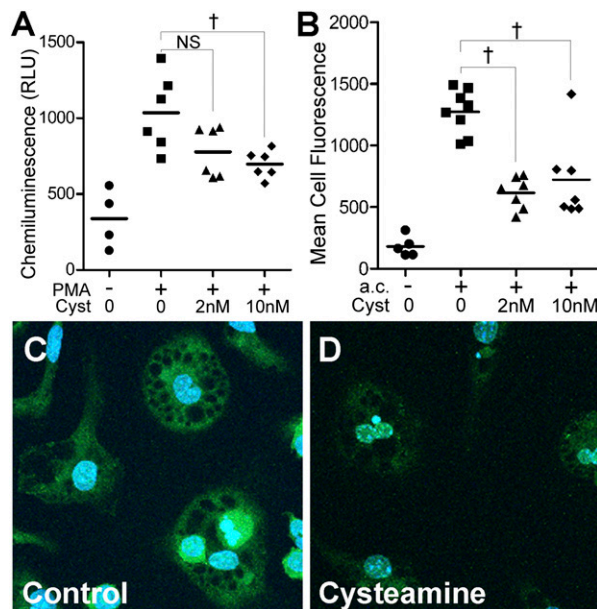


**Figure 6.** ROS generation is diminished with cysteamine treatment in two *in vitro* models of oxidant stress. (A) Phorbol-induced oxidant stress. RAW macrophages are incubated with or without cysteamine for 60 minutes before the addition of 10  $\mu$ M of PMA and the chemiluminescence agent. The graph summarizes the results of extracellular ROS released ( $n=4-6$  per group). (B–D) Apoptotic cell phagocytosis-induced oxidant stress. Thiolglycollate-elicited mouse peritoneal macrophages are cultured with or without cysteamine for 24 hours. Late-stage apoptotic tubular cells are generated by irradiating mouse cortical tubular cells and cocultured with control or cysteamine-treated peritoneal macrophages for 24 hours before being treated with CellRox (green). Nuclei are counterstained with TO-PRO (blue). (B) The graph summarizes the semiquantitative results of mean macrophage oxidant species. (C and D) Representative macrophage oxidation images are shown for control and cysteamine-treated macrophages.  $^{\dagger}P<0.01$ ;  $^{\ddagger}P<0.05$ , control versus cysteamine-treated groups. RLU, relative light unit; MCT, mouse cortical tubular cell.

were similar in the cysteamine-treated and control mice on days 7 and 14, suggesting that cysteamine modulates interstitial myofibroblast accumulation *via* a mechanism that is independent of the classic TGF- $\beta$  fibrogenic signaling pathway (Supplemental Figure 2).

#### Cysteamine Blocks Myofibroblast Proliferation

(Myo)fibroblast proliferation is an essential feature of the wound healing response that typifies renal fibrosis. Proliferating cells were labeled *in vivo* by injecting bromodeoxyuridine (BrdU) the day before euthanasia. The number of BrdU+ tubulointerstitial cells detected immunohistochemically was significantly reduced by 49% on day 7 in cysteamine-treated mice compared with controls, but no difference was observed

at day 14 (Figure 8, A–C). When the number of cells expressing the proliferation marker Ki67 was enumerated by confocal microscopy, a significant 27% reduction was confirmed on day 7. Dual staining confocal microscopy further established that the cellular proliferation changes were largely driven by a significant 65% reduction in proliferating myofibroblasts (Ki67+ plus  $\alpha$ SMA+ cells) in cysteamine-treated mice compared with controls (Figure 8, D–F).

Although recent studies suggest that pericytes positive for PDGF receptors (PDGF-Rs)  $\alpha$  and  $\beta$  are an important source of the interstitial myofibroblast population in CKD,<sup>23</sup> significant differences in kidney PDGF-R $\alpha$  and PDGF-R $\beta$  mRNA levels were not detected in cysteamine-treated mice compared with controls at any time point (Supplemental Table 2).

#### Cysteamine Inhibits Myofibroblast Proliferation and Activation *In Vitro*

To further explore the possible effects of cysteamine on myofibroblast generation, the well established *in vitro* model of TGF- $\beta$ -dependent fibroblast-to-myofibroblast differentiation was utilized.<sup>24,25</sup> To determine the effect of cysteamine on myofibroblast proliferation, TGF- $\beta$ -stimulated NRK-49F cells were placed in growth-promoting conditions with two different concentrations of cysteamine (0.5 nM and 2 nM). Exposure to cysteamine at both concentrations led to a nearly 50% reduction in myofibroblast cell proliferation rates at 24 hours and 30% at 48 hours (Figure 9, A and B). The effect of cysteamine exposure on cell viability was nonsignificant (5%–7% nonviable cells,  $P=0.26$ , Figure 9C). To determine whether the antiproliferative effect of cysteamine on myofibroblasts was cell type specific, murine proximal tubular cells were incubated under growth-promoting conditions in the presence or absence of cysteamine. In contrast to the observed effects on transformed NRK cells, there was no difference in proximal tubular cell proliferation rates with the 0.5 nM or 2 nM cysteamine dose at 24 hours (Figure 9D).

Although we did not see any changes in PDGF-R transcription, we further sought to determine whether cysteamine had antiproliferative effects on pericyte-derived myofibroblasts. Primary pericytes were isolated from normal kidneys as previously described<sup>26</sup> and cultured in growth media with TGF- $\beta$  in the presence or absence of cysteamine for 24 hours. Previous studies demonstrate that primary pericytes treated with TGF- $\beta$  express  $\alpha$ SMA after 24 hours.<sup>26</sup> Similar to our findings on NRK cells, we found that there was a 70% reduction in pericyte-derived myofibroblasts with cysteamine treatment (Figure 10).

To determine the effect of cysteamine on myofibroblast differentiation and activation, NRK-49F cells were grown under low serum conditions and exposed to TGF- $\beta$  to induce  $\alpha$ SMA expression. Cysteamine treatment (2 nM) induced a significant 70% reduction in  $\alpha$ SMA mRNA levels and a 52% reduction in  $\alpha$ SMA

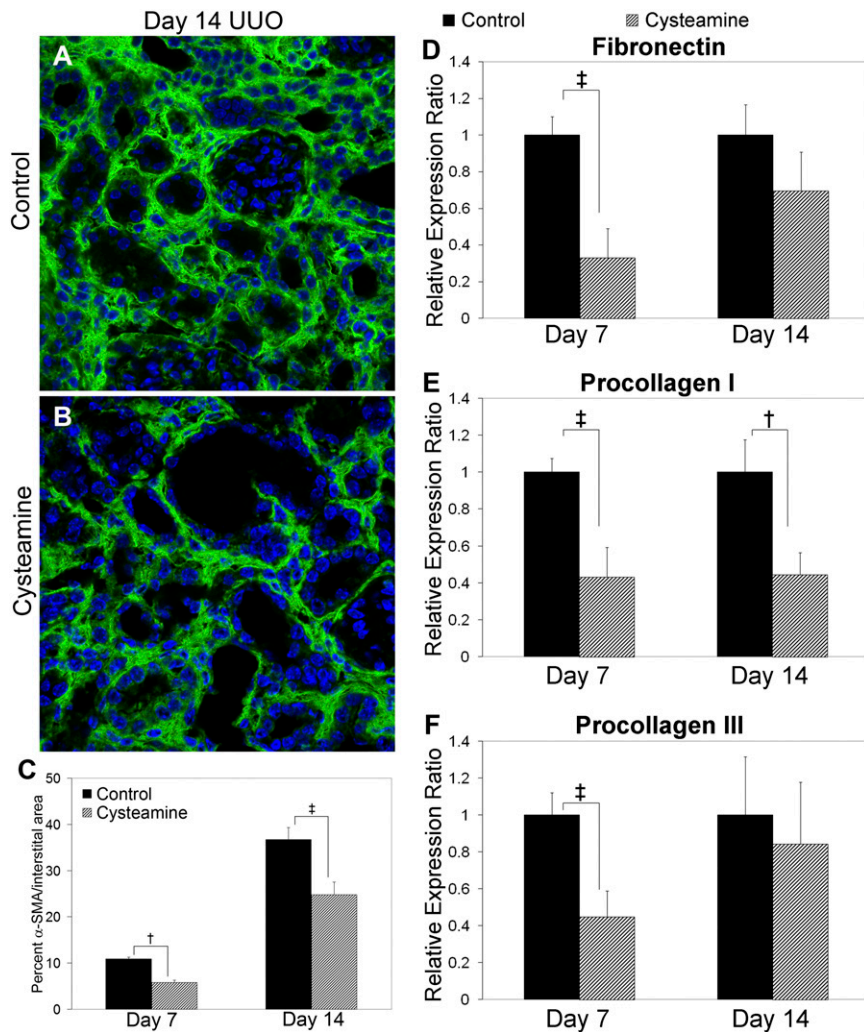


**Figure 7.** Interstitial myofibroblast accumulation is attenuated with cysteamine treatment. (A and B) Representative  $\alpha$ SMA-stained confocal images are shown for day 14 UOU. (C) The graph summarizes the semiquantitative results of the analysis of the tubulointerstitial area expressing  $\alpha$ SMA protein ( $n=7-8$  per group). (D-F) The graphs show the results of analysis of kidney ECM mRNA levels, measured by semiquantitative real-time PCR and normalized to two housekeeping genes, 18S and GAPDH. (D) Fibronectin. (E) Procollagen I. (F) Procollagen III. Results are expressed as the mean  $\pm$  SEM.  $^{\dagger}P<0.01$ ;  $^{\ddagger}P<0.05$ , control versus cysteamine-treated groups. Original magnification,  $\times 400$ .

protein expression compared with controls (Figure 9, E and F). No differences were detected in the 0.5 nM cysteamine group, suggesting a dose-dependent effect of cysteamine on myofibroblast differentiation. A recent study demonstrated that TGF- $\beta$  induces expression of Nox4, an enzyme that generates hydrogen peroxide in fibroblasts, via Smad3 and that this is an important pathway in myofibroblast differentiation.<sup>27</sup> In this study, cysteamine treatment did not alter Nox4 mRNA levels

and there was no difference in phosphorylated-Smad3 by Western blot (Supplemental Figure 3). Collectively, these data suggest that cysteamine bitartrate specifically targets and inhibits the proliferation and activation of myofibroblasts.

#### Cysteamine Attenuates CKD after AKI

To determine whether cysteamine also attenuated fibrosis when it was started a period of time after the onset of kidney

injury, a study was performed in a model of ischemia reperfusion injury (IRI) in C57BL/6 mice. We started 600 mg/kg of cysteamine bitartrate 10 days after surgery and continued the treatment for 14 days. We found that there was a 40% reduction in fibrosis severity and a 75%–82% reduction in ECM mRNA levels with cysteamine treatment after IRI (Figure 11). These studies strongly suggest that cysteamine has therapeutic potential in preventing CKD progression after kidney injury.

#### DISCUSSION

Despite the huge disease burden associated with human CKD, there are few known therapeutic options that have a clinically significant effect on disease progression rates beyond blockade of the renin-angiotensin system and there are no currently approved therapies that stop or reverse it. The remarkable efficacy of cysteamine bitartrate (Cystagon) in the treatment of nephropathic cystinosis led us to investigate its efficacy as an antifibrotic agent in two well established experimental models of kidney fibrosis: UOU and IRI. This study is the first to report the ability of cysteamine to significantly attenuate renal fibrosis in the setting of chronic injury not associated with cystinosis and further demonstrates its antifibrotic efficacy when initiated several days after the onset of AKI. In a small pilot study in children with non-alcoholic fatty acid liver disease, cysteamine was reported to normalize liver function tests, but liver histology was not available to determine whether hepatic fibrosis was attenuated.<sup>13,14</sup> Although the drug was added to the drinking water in this study and thus the delivered doses are estimated and are much higher than typically administered to humans (typically 30–50 mg/kg per day), the observed peak plasma levels in this study (15–20  $\mu$ M) were comparable with those observed in cystinotic patients. Due to the short  $t_{1/2}$  of cysteamine (94–114 min<sup>28,29</sup>), “therapeutic” cysteamine levels were only observed overnight while the animals were drinking. Despite this

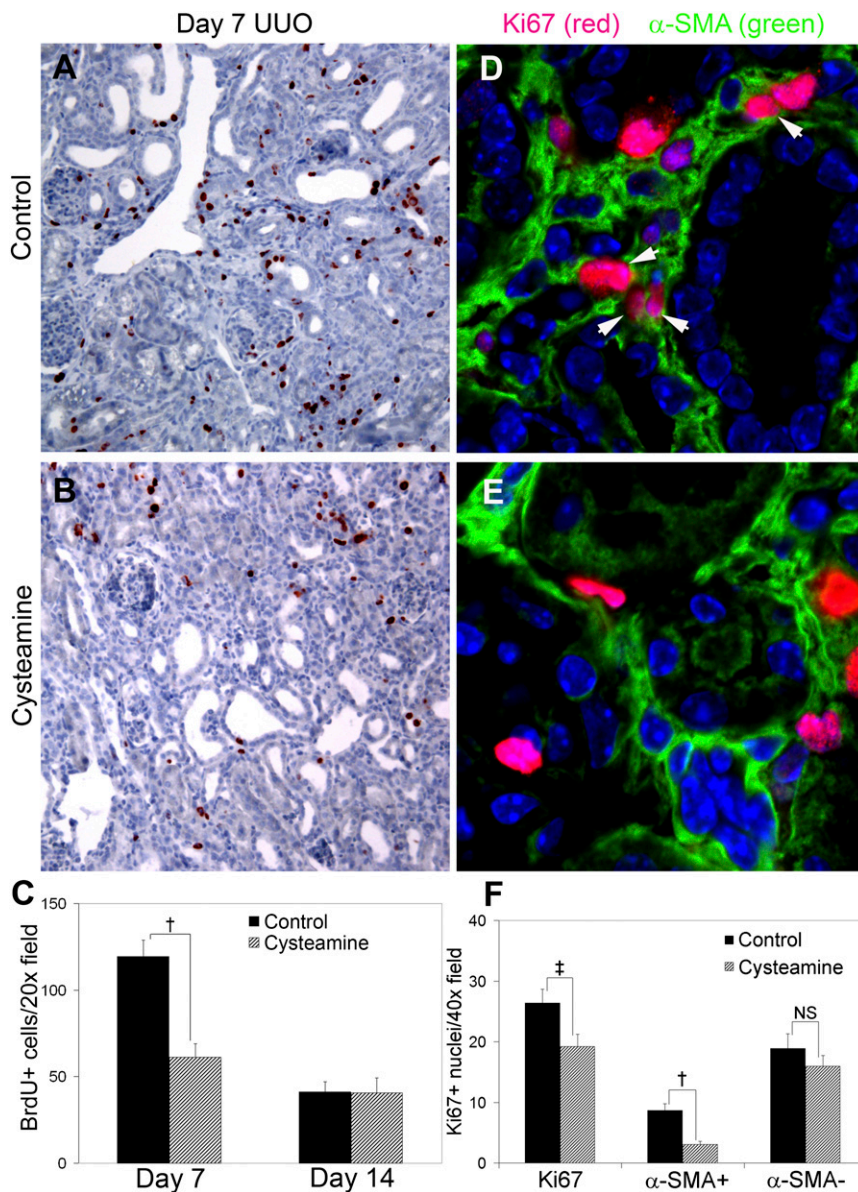


**Figure 8.** Myfibroblast proliferation is decreased in cysteamine-treated mice. (A and B) Mice are injected with BrdU the day before euthanasia. Representative immunohistochemical photomicrographs on the left illustrate BrdU+ cells identified by the brown stain; nuclei are counterstained with hematoxylin. (C) The graph summarizes the results of the semiquantitative analysis of the number of proliferating BrdU+ tubulointerstitial cells ( $n=5-8$  per group). (D and E) Dual staining confocal microscopy is performed with anti- $\alpha$ SMA (green) and anti-Ki67 (red) primary antibodies and magnified photomicrographs are shown on the right. The number of double-positive cells (arrow) is counted in six randomly selected fields from each experimental animal ( $n=8$  animals per group). (F) The lower right graph summarizes the results, showing the significant differences in the total number of Ki67+ cells and Ki67 plus  $\alpha$ SMA+ cells. All results are expressed as the mean  $\pm$  SEM.  $^{\dagger}P<0.01$ ;  $^{\ddagger}P<0.05$ , control versus cysteamine-treated groups. NS, not significant. Original magnification,  $\times 200$  in A and B;  $\times 400$  in D and E.

limitation, a significant antifibrotic effect was observed. It is possible that an even greater fibrosis-attenuating effect might be achieved if levels are sustained in the

therapeutic range. The limitation of the short  $t_{1/2}$  and need for frequent dosing was recently addressed by the production of an enteric-coated formulation that

appears to have similar efficacy in cystinotic patients despite a 50% reduction in the number of daily doses.<sup>15,30,31</sup> It should be noted that drug concentrations in the 0.5–2 nM range that were used for the *in vitro* studies are pharmacologically relevant based on the human data.

An important question is the mechanistic basis of the antifibrotic effects that were associated with cysteamine therapy. The results of this study provide some insights, highlighting the antioxidant properties and direct effects of cysteamine on myfibroblast differentiation and proliferation. There is a substantial body of evidence supporting the hypothesis that increased oxidative stress plays an important role in the development of fibrotic diseases in humans.<sup>5,32,33</sup> Prior studies centered on the reduction of oxidized macromolecules as the critical component to limiting disease progression,<sup>34,35</sup> rather than the specific redox-sensitive pathways or target cells that are directly modulated by antioxidants.<sup>36,37</sup> We found that cysteamine bitartrate treatment resulted in a substantial reduction in protein oxidation (>50%) despite no change in total thiol levels at advanced time points. These results, combined with our *in vitro* studies, suggest that the cysteamine-dependent antioxidant mechanism was not simply due to a drug-derived increase in the free thiol cellular pool; rather, its downstream modulatory effects on oxidant-generating pathways attenuated tissue damage.

The lynchpin of the renal fibrogenic response is the *de novo* appearance of a unique population of cells that are typically identified by their interstitial location, their fibroblastic appearance, and their expression of  $\alpha$ SMA. These cells are the primary source of the scar-generating ECM proteins that accumulate within the interstitial space and lead to progressive nephron loss and renal functional deterioration. Therapy that selectively targets myfibroblast generation and/or activation is an attractive antifibrotic strategy. Identifying such therapies is complicated by the fact that there appear to be several cellular origins for interstitial myfibroblasts and they appear

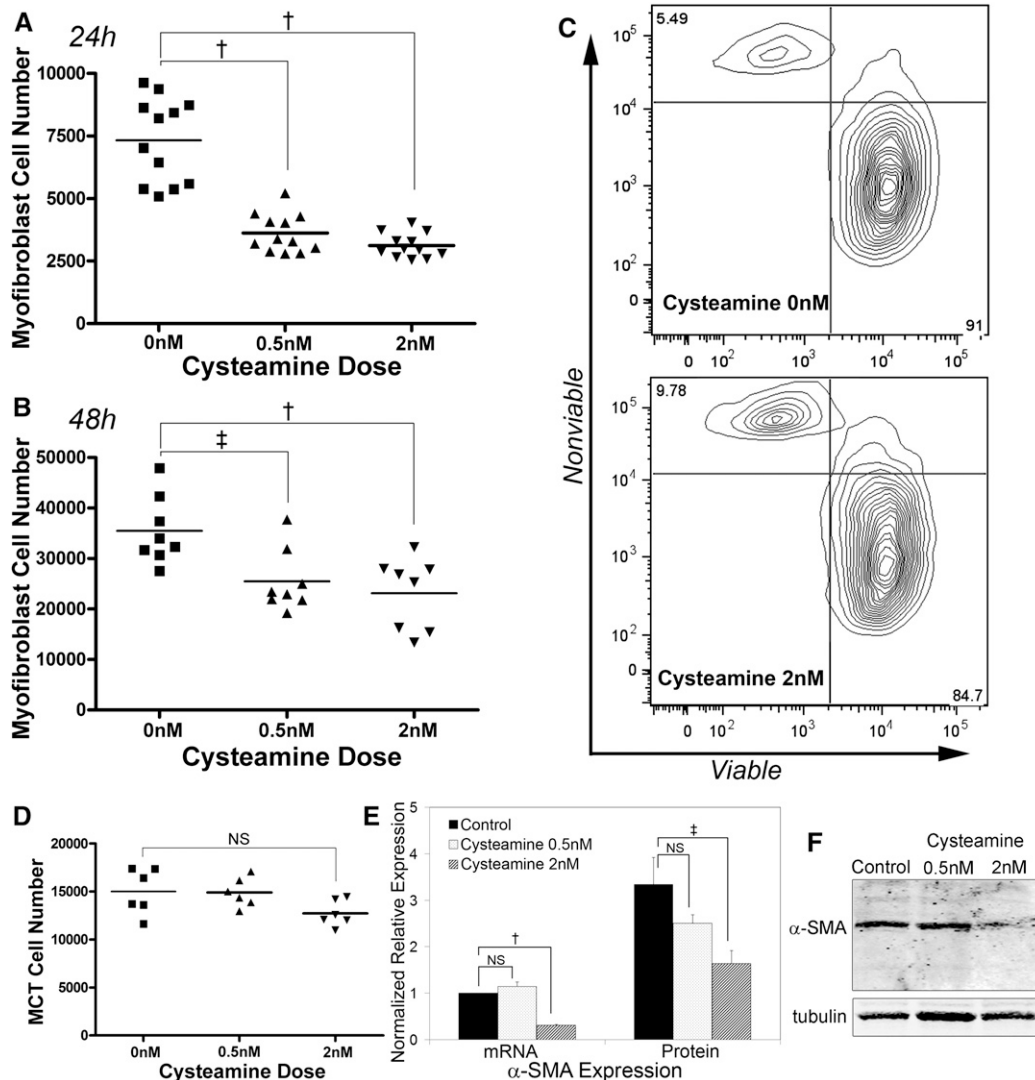


**Figure 9.** Cysteamine blocks both myofibroblast proliferation and activation. Normal rat kidney fibroblasts (NRK-49F) are transformed into  $\alpha$ SMA+ myofibroblasts by exposure to TGF- $\beta$ . For proliferation experiments, cells are placed in growth media plus TGF- $\beta$  with cysteine or vehicle alone. (A and B) The graphs show the number of myofibroblasts and illustrate significantly reduced proliferation rates with cysteine treatment at both 24 hours (A) and 48 hours (B). (C) Representative FACS plots illustrate similar numbers of viable NRK-49F cells after cysteine exposure, as measured by reaction with the polyanionic dye calcein and FACS analysis ( $n=3$  per group). (D) Mouse proximal tubular cells incubated in growth media in the absence (0 nM) or presence of cysteine (0.5 and 2 nM) show similar proliferation rates at 24 hours ( $n=6$ ). (E) The graph summarizes the results of effects of cysteine on the differentiation of NRK-49F fibroblasts into  $\alpha$ SMA+ myofibroblasts as assessed by mRNA levels measured by semiquantitative real-time PCR and protein levels measured by Western blotting ( $n=4$  per group). (F) A representative  $\alpha$ SMA Western blot. Results are expressed as the mean  $\pm$  SEM.  $\dagger P<0.01$ ;  $\ddagger P<0.05$ , control versus cysteine-treated cells. NS, not significant.

to be functionally heterogeneous.<sup>38</sup> Our data suggest that cysteine blocks kidney fibroblast responses to chronic injury. Both the *in vivo* and *in vitro* data confirmed a significant reduction in interstitial myofibroblast numbers coupled with reduced (myo)fibroblast mitotic activity. The functional consequence of these changes is reduced ECM protein

mRNA levels, suggesting that fibrosis attenuation was a consequence of less interstitial matrix synthesis. Although a broad screen of several cell types was not performed, failure of cysteine to inhibit tubular cell proliferation suggests that its antimitotic activity could be selective for (myo)fibroblasts. Recent studies by Duffield *et al.* highlighted pericytes as

an important source of myofibroblasts and provided evidence that their detachment from endothelial cells is an early event after kidney injury (days 1–5 after UUO).<sup>23,39–41</sup> Although we did not detect any changes in whole kidney PDGF-R mRNA expression, our *in vitro* data suggest that cysteine has antimitotic effects on both fibroblasts and activated pericytes.

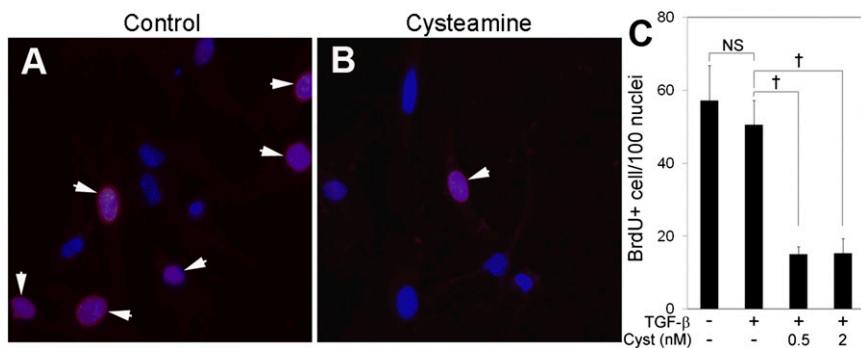


**Figure 10.** Cysteamine blocks pericyte-derived myfibroblast proliferation. PDGFR- $\beta$ + pericytes are isolated from normal mouse kidneys and cultured in the presence of TGF- $\beta$  in growth media with or without cysteamine for 24 hours; cells are treated with BrdU before fixation. (A and B) Representative fluorescent images of control and cysteamine-treated pericyte-derived myfibroblasts. BrdU (red), nuclei (blue). White arrowheads highlight double-positive cells. (C) The graph summarizes the semiquantitative results of BrdU+ proliferating myofibroblasts. Results are expressed as the mean  $\pm$  SEM.  $^{\dagger}P < 0.01$ , control versus cysteamine-treated cells. NS, not significant,

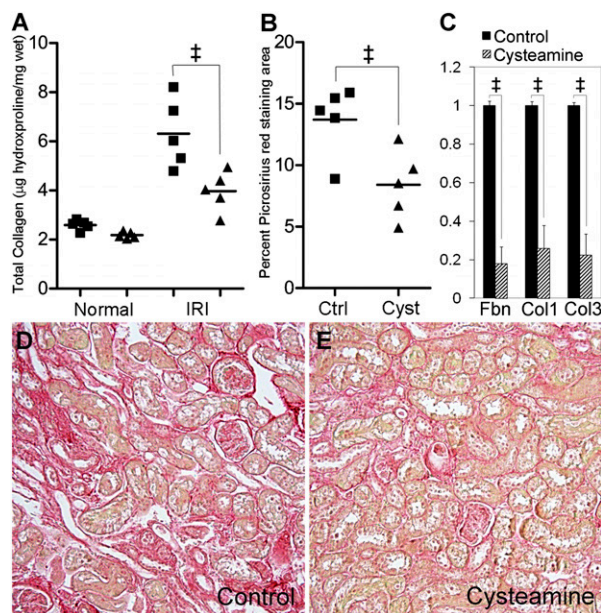


**Figure 11.** Cysteamine attenuates fibrosis progression after AKI. Unilateral IRI is induced. Cysteamine bitartrate is started 10 days after surgery and continues for 14 days until euthanasia. (A) The graph summarizes fibrosis severity after IRI, shown as the total kidney collagen content, measured using the hydroxyproline assay, in the group of cysteamine-treated mice (black triangles) compared with the control group (black squares) ( $n = 5$  mice per group). (B) The graph summarizes the results of picrosirius red-positive interstitial collagen quantification, with representative light photomicrographs (D and E) that confirm diminished matrix deposition. (C) The graph summarizes the results of the analysis of kidney ECM mRNA levels, measured by semiquantitative real-time PCR and normalized to two housekeeping genes, 18S and GAPDH. Results are expressed as the mean  $\pm$  SEM.  $^{\ddagger}P < 0.05$ , control versus cysteamine-treated groups. FBN, fibronectin; Col1, procollagen I; Col3, procollagen III. Original magnification,  $\times 400$  in D and E.

The effects of cysteamine on (myo) fibroblasts were further substantiated by *in vitro* experiments that used TGF- $\beta$  exposure to stimulate  $\alpha$ SMA expression in normal kidney fibroblasts and pericytes. The ability of cysteamine to inhibit cell proliferation was most striking during the first 24 hours, suggesting that it may have affected specific rates of cell cycle entry or mitogenic signaling pathways that are currently under investigation. An intriguing observation suggests that the effects of cysteamine may be independent of the classic TGF- $\beta$ -Smad3 fibrogenic pathway, given that both the *in vivo* and *in vitro* experiments failed to detect significant differences in phospho-Smad3 levels. Although recent studies report that Nox4-dependent generation of hydrogen peroxide is essential for TGF- $\beta$ -induced myofibroblast differentiation,<sup>27,42,43</sup> the results of this study suggest that cysteamine inhibited myofibroblast differentiation *via* a Nox4- and Smad3-independent pathway. We postulate that cysteamine modifies TGF- $\beta$ -induced myofibroblast differentiation *via* an alternative redox-regulated mechanism that requires further investigation.

Cysteamine bitartrate almost certainly influences additional reactions that are relevant to its antifibrotic effects. For example, the number of F4/80+ interstitial macrophages was significantly reduced, but it is not clear whether this was a primary effect or a downstream consequence of reduced kidney damage. On the basis of preliminary whole kidney cytokine and oxidant gene profiling studies, cysteamine therapy did not significantly modify functional secretory products that are typically associated with macrophage polarity. However, the likely contribution of other kidney cells to these levels does not allow us to definitively conclude that cysteamine failed to alter the macrophage functional profile. The possible renoprotective action of cysteamine as a Tgm2 inhibitor was not supported by measurable differences in whole kidney transglutaminase activity. A recent study confirms that cysteamine enters the lysosome and combines with cystine to form a mixed

disulfide that resembles lysine and is transported out of the lysosome<sup>44</sup>; however, it is not clear whether lysosomal cystine accumulation occurs during tissue injury and its contribution to fibrogenesis has yet to be defined. Alternatively, several studies demonstrated the importance of cystine–cysteine balance in the modulation of redox signaling<sup>45–47</sup> and the relative contribution of this mechanism toward the antifibrotic potential of cysteamine is under investigation.

In summary, cysteamine bitartrate had impressive antifibrotic effects *in vivo*, even when a drug delivery system was used that only achieved “therapeutic” serum levels for <50% of the day. Biologically plausible antifibrotic mechanisms of action that were supported by the results of studies using *in vivo* and *in vitro* models of kidney fibrosis identified effects on (myo)fibroblast activity. Further studies are justified to validate these findings in anticipation of future therapeutic trials in human CKD.

## CONCISE METHODS

### Experimental Design

Wild-type C57BL/6 male mice, aged 8–10 weeks, were purchased from Jackson Laboratory. UUO was performed as previously described on wild-type male mice, aged 8–10 weeks ( $n=6–10$  each), and they were euthanized at 3, 7, 14, and 21 days after surgery. Unilateral IRI surgery was performed through a retroperitoneal, paraspinal incision and placement of a vascular clamp on the left renal pedicle for 28 minutes while mice were kept at a constant temperature of 37°C using a rectal probe temperature controller (Braintree Scientific). Reperfusion was confirmed with release of the vascular clamp and mice were given a 1-ml intraperitoneal injection of warm saline at the conclusion of the procedure. All procedures were performed in accordance with the guidelines established by the National Research Council Guide for the Care and Use of Laboratory Animals and were approved by our Institute Animal Care and Use Committee. Cysteamine bitartrate (600 mg/kg; Cystagon) was added to the drinking water on the day of

UUO surgery or 10 days after IRI surgery, protected from light, and changed daily throughout the duration of the study. It was assumed that an average 25-g mouse would drink 5 ml of water per day. Contralateral and UUO kidneys were harvested and processed for RNA and protein extraction and histologic studies as previously described.<sup>19,20,48</sup> Frozen tissue samples were stored at  $-80^{\circ}\text{C}$ .

### Collagen Content

Hydroxyproline content of kidney tissue (micrograms of hydroxyproline per milligram of wet weight kidney section) was measured by acid hydrolysis of the tissue section using procedures established in our laboratory.<sup>19,20,48</sup>

### Histologic Examination

Immunohistochemical staining was performed on sections of paraffin-embedded tissue or cryosections of snap-frozen tissue using procedures established in our laboratory with VECTASTAIN *Elite* ABC Kits (Vector Laboratories Inc.) and AEC Substrate Chromogen K3464 (Dako Corp.). Sections were blocked with a Avidin/Biotin blocking kit (Vector Laboratories Inc.). Confocal microscopy was performed on 5- $\mu\text{m}$  cryosections fixed with 4% paraformaldehyde and imaged with the Leica SP5 confocal microscope. In some cases, tyramide signal amplification was utilized (TSA kit #3-488 tyramide and TSA kit #4-546 tyramide; Invitrogen). Nuclei were stained with TO-PRO-3 iodide. Primary antibodies used were reactive with F4/80 (rat anti-mouse F4/80 monoclonal-Cy3; AbD Serotec),  $\alpha\text{SMA}$  (mouse anti-mouse monoclonal  $\alpha\text{SMA}$ -FITC; Sigma-Aldrich), BrdU (rabbit anti-BrdU), Ki67 (rabbit anti-human Ki67; Abcam), and phosphorylated Smad3 (rabbit anti-human phospho-Smad3 monoclonal; Cell Signaling Technology). Picrosirius red staining was performed as previously described.<sup>20,48</sup> Secondary antibodies were shown to be nonreactive with tissue sections stained without the primary antibody. Semiquantitative computer-assisted image analysis was performed with Image-Pro Plus software (Mediatech) on 6–8 randomly selected  $\times 400$  magnified images of slides from individual animals. Interstitial macrophage and myofibroblast densities were expressed as the percentage of F4/80+ and  $\alpha\text{SMA}$  interstitial

area on fluorescent-stained cryosections. The investigator was blinded to the experimental groups at the time of analysis.

### Western Blotting

Protein was isolated from homogenized frozen kidneys and Western blotting was performed as previously described.<sup>19,20</sup> The primary antibodies are described above. Bands were normalized using  $\alpha$ -tubulin (anti-mouse  $\alpha$ -tubulin; Abcam). The secondary antibodies were IR700Dye and IR800Dye (Rockland Immunochemicals Inc.). Protein bands were visualized and quantified using the Odyssey imaging system (Li-Cor Biosciences).

### Semiquantitative Real-Time PCR

Total RNA from frozen kidney tissue homogenate was obtained using the Maxwell 16 instrument (Promega). RNA samples were loaded on a Agilent RNA 6000 Nano Chip and analyzed in the Agilent 2100 Bioanalyzer (Agilent Technologies) for RNA concentration and quality; samples with RNA integrity numbers  $>8.0$  were utilized for cDNA synthesis. First-strand cDNA was prepared from 1  $\mu\text{g}$  of total RNA using the Bio-Rad iScript cDNA Synthesis kit (Bio-Rad Laboratories). Semiquantitative real-time PCR was performed according to the IQ SYBR Green Supermix kit methods (Bio-Rad Laboratories) using primers (see Supplemental Table 3), as previously described.<sup>20</sup> Reactions were run in triplicate and genes of interest were normalized to both 18S and GAPDH housekeeping genes. Data analysis was performed using the Pfaffl algorithm with REST analysis software (version 1.9.9; Corbett Research Pty Ltd).

### Oxidative Stress and Transglutaminase Activity

Total kidney protein was processed in a modified radioimmunoprecipitation assay buffer with thiol inhibitors. Total thiols were measured using the Measure-IT Thiol kit (Invitrogen). Carbonyl protein levels were measured by ELISA (OxiSelect). Transglutaminase activity was measured using the Transglutaminase Assay Kit (Sigma-Aldrich). Samples were performed in triplicate.

**Macrophage ROS Production and Phagocytosis**  
RAW 264.7 macrophage cell lines (ATCC) were harvested and placed in HBSS media at

$10^6$  cells/ml with cysteamine bitartrate or vehicle alone for 1 hour at 37°C. We added 10  $\mu$ M of PMA (Sigma) and 0.5 mM of L-012 (WAKO) to 100  $\mu$ l of cells in a 96-well plate and luminescence was measured in the SpectraMax 190 microplate reader (Molecular Devices).

Apoptotic renal tubular cells were generated by irradiating (20 Gy) immortalized murine proximal tubular cells at 60%–70% confluency in DMEM with 5% FCS (media) to induce apoptosis. Apoptosis was confirmed by Annexin V FACS analysis and DNA fragmentation assays. Thioglycollate-elicited macrophages were harvested 3 days after intraperitoneal injection of 3% thioglycollate (Fisher Scientific) and cultured for 24 hours in media with or without cysteamine. Thioglycollate-elicited macrophages were cocultured with apoptotic murine proximal tubular cells (24 hours after irradiation) at a 3:1 ratio (apoptotic cell/macrophage). After 4 hours, cells were washed with PBS to remove nonphagocytosed cells and placed in media with or without cysteamine. After 24 hours, macrophages were treated with CellRox 480 (Invitrogen) according to the manufacturer's protocol and fixed and the nuclei were counterstained with TO-PRO. Fluorescent z-stack images were obtained by confocal microscopy (Leica SP5) in eight randomly selected fields and compressed into a single image. Oxidative products were measured by computer-assisted image analysis in each macrophage and the mean macrophage oxidative product generation (mean cell fluorescence) was calculated for each field.

Phagocytosis efficiency was measured using pHrodo *Escherichia coli* BioParticles (Invitrogen) in bone marrow–derived macrophages according to the manufacturer's protocol. Bone marrow was harvested from femurs and tibias of wild-type C57BL/6 mice and cultured in petri dishes with DMEM, 10% FCS, supplemented with 0.1  $\mu$ g/ml of macrophage colony stimulating factor for at least 6 days. Bone marrow–derived macrophages were used between 6 and 8 days. Each experiment was repeated in triplicate.

### In Vitro Myofibroblast Studies

Normal rat kidney fibroblasts (NRK-49F) were purchased from ATCC. Recombinant human TGF- $\beta$  dose-response experiments determined the optimal dose to transform NRK cells to  $\alpha$ SMA+ myofibroblasts using  $\alpha$ SMA

Western blotting as the readout. For investigation of myofibroblast activation, NRK cells were seeded at 50% confluency and placed in low serum media (DMEM, 1% FCS) with 2.5 ng/ml of TGF- $\beta$  for 48 hours. TGF- $\beta$  and cysteamine were changed daily.  $\alpha$ SMA protein and mRNA levels were measured by Western blot and semiquantitative real-time PCR, respectively. For investigation of myofibroblast proliferation, NRK cells were seeded at 50% confluency, grown in low serum media for 6 hours, and then placed in growth media (DMEM, 5% FCS) with 2.5 ng/ml of TGF- $\beta$ . The cell number was measured using the CyQuant kit (Invitrogen) at 24 and 48 hours (85%–90% confluency). Cell viability was confirmed by FACS analysis using the Live/Dead Viability/Cytotoxicity Kit (Invitrogen).

Primary pericytes were obtained from normal kidneys from wild-type C57BL/6 mice as previously described,<sup>26</sup> and cultured on coverslips. Pericytes were serum deprived for 24 hours before being placed in media with cysteamine bitartrate or vehicle alone for 24 hours. Cells were pulsed with BrdU 6 hours before fixation. Cells were permeabilized and stained with rat anti-BrdU followed by secondary donkey anti-rat Cy3. Eight randomly selected fields were chosen and the number of BrdU+ nuclei was enumerated for control and cysteamine-treated cells. Each experiment was repeated in triplicate.

### Statistical Analyses

All data are presented as the mean  $\pm$  SEM. A nested ANOVA was utilized for all semiquantitative computer-assisted image analysis data. For the latter, the arithmetic mean of six randomly selected images of slides for each animal was used to calculate the reported mean of the group and the SEM. All other results were analyzed by the unpaired *t* test. Nonparametric data were analyzed using the Mann–Whitney *U* test. *F* statistic values are reported for all ANOVAs and *z* values are reported for Mann–Whitney tests. A *P* value <0.05 was considered statistically significant. Some graphs were generated using GraphPad Prism software.

### ACKNOWLEDGMENTS

We thank Dr. Jerry Schneider for encouraging us to investigate the effects of cysteamine on renal fibrosis.

This investigation was supported wholly by a grant from the Cystinosis Research Foundation.

### DISCLOSURES

None.

### REFERENCES

1. Taguchi K, Fujikawa N, Komatsu M, Ishii T, Unno M, Akaike T, Motohashi H, Yamamoto M: Keap1 degradation by autophagy for the maintenance of redox homeostasis. *Proc Natl Acad Sci U S A* 109: 13561–13566, 2012
2. Churchman AT, Anwar AA, Li FY, Sato H, Ishii T, Mann GE, Siow RC: Transforming growth factor-beta1 elicits Nrf2-mediated antioxidant responses in aortic smooth muscle cells. *J Cell Mol Med* 13: 2282–2292, 2009
3. Yoo SK, Starnes TW, Deng Q, Huttenlocher A: Lyn is a redox sensor that mediates leukocyte wound attraction in vivo. *Nature* 480: 109–112, 2011
4. Latchoumycandane C, Marathe GK, Zhang R, McIntyre TM: Oxidatively truncated phospholipids are required agents of tumor necrosis factor  $\alpha$  (TNF $\alpha$ )-induced apoptosis. *J Biol Chem* 287: 17693–17705, 2012
5. Okamura DM, Himmelfarb J: Tipping the redox balance of oxidative stress in fibrogenic pathways in chronic kidney disease. *Pediatr Nephrol* 24: 2309–2319, 2009
6. Benigni A, Corna D, Zoja C, Sonzogno A, Latini R, Salio M, Conti S, Rottoli D, Longaretti L, Cassis P, Morigi M, Coffman TM, Remuzzi G: Disruption of the Ang II type 1 receptor promotes longevity in mice. *J Clin Invest* 119: 524–530, 2009
7. Johnson-Davis KL, Fernelius C, Eliason NB, Wilson A, Beddhu S, Roberts WL: Blood enzymes and oxidative stress in chronic kidney disease: A cross sectional study. *Ann Clin Lab Sci* 41: 331–339, 2011
8. Small DM, Coombes JS, Bennett N, Johnson DW, Gobe GC: Oxidative stress, anti-oxidant therapies and chronic kidney disease. *Nephrology (Carlton)* 17: 311–321, 2012
9. Gahl WA, Balog JZ, Kleta R: Nephropathic cystinosis in adults: Natural history and effects of oral cysteamine therapy. *Ann Intern Med* 147: 242–250, 2007
10. Greco M, Brugnara M, Zaffanello M, Taranta A, Pastore A, Emma F: Long-term outcome of nephropathic cystinosis: A 20-year single-center experience. *Pediatr Nephrol* 25: 2459–2467, 2010
11. Borrell-Pagès M, Canals JM, Cordelières FP, Parker JA, Pineda JR, Grange G, Bryson EA, Guillemier M, Hirsch E, Hantraye P, Cheetham ME, Néri C, Alberch J, Brouillet E, Saudou F, Humbert S: Cystamine and cysteamine increase brain levels of BDNF in Huntington disease via HSP1b and transglutaminase. *J Clin Invest* 116: 1410–1424, 2006

12. Fujisawa T, Rubin B, Suzuki A, Patel PS, Gahl WA, Joshi BH, Puri RK: Cysteamine suppresses invasion, metastasis and prolongs survival by inhibiting matrix metalloproteinases in a mouse model of human pancreatic cancer. *PLoS ONE* 7: e34437, 2012
13. Dohil R, Meyer L, Schmeltzer S, Cabrera BL, Lavine JE, Phillips SA: The effect of cysteamine bitartrate on adiponectin multimerization in non-alcoholic fatty liver disease and healthy subjects. *J Pediatr* 161: 639–645.e1, 2012
14. Dohil R, Schmeltzer S, Cabrera BL, Wang T, Durelle J, Duke KB, Schwimmer JB, Lavine JE: Enteric-coated cysteamine for the treatment of paediatric non-alcoholic fatty liver disease. *Aliment Pharmacol Ther* 33: 1036–1044, 2011
15. Dohil R, Fidler M, Barshop BA, Gangoiti J, Deutsch R, Martin M, Schneider JA: Understanding intestinal cysteamine bitartrate absorption. *J Pediatr* 148: 764–769, 2006
16. Johnson TS, Fisher M, Haylor JL, Hau Z, Skill NJ, Jones R, Saint R, Coutts I, Vickers ME, El Nahas AM, Griffin M: Transglutaminase inhibition reduces fibrosis and preserves function in experimental chronic kidney disease. *J Am Soc Nephrol* 18: 3078–3088, 2007
17. Johnson TS, Griffin M, Thomas GL, Skill J, Cox A, Yang B, Nicholas B, Birckbichler PJ, Muchaneta-Kubara C, Meguid El Nahas A: The role of transglutaminase in the rat subtotal nephrectomy model of renal fibrosis. *J Clin Invest* 99: 2950–2960, 1997
18. Johnson TS, Skill NJ, El Nahas AM, Oldroyd SD, Thomas GL, Douthwaite JA, Haylor JL, Griffin M: Transglutaminase transcription and antigen translocation in experimental renal scarring. *J Am Soc Nephrol* 10: 2146–2157, 1999
19. Okamura DM, López-Guisa JM, Koelsch K, Collins S, Eddy AA: Atherogenic scavenger receptor modulation in the tubulointerstitium in response to chronic renal injury. *Am J Physiol Renal Physiol* 293: F575–F585, 2007
20. Okamura DM, Pennathur S, Pasichnyk K, López-Guisa JM, Collins S, Febbraio M, Heinecke J, Eddy AA: CD36 regulates oxidative stress and inflammation in hypercholesterolemic CKD. *J Am Soc Nephrol* 20: 495–505, 2009
21. Deschacht M, Horemans T, Martinet W, Bult H, Maes L, Cos P: Comparative EPR study of different macrophage types stimulated for superoxide and nitric oxide production. *Free Radic Res* 44: 763–772, 2010
22. Kopprasch S, Pietzsch J, Graessler J: Validation of different chemiluminescent substrates for detecting extracellular generation of reactive oxygen species by phagocytes and endothelial cells. *Luminescence* 18: 268–273, 2003
23. Chen YT, Chang FC, Wu CF, Chou YH, Hsu HL, Chiang WC, Shen J, Chen YM, Wu KD, Tsai TJ, Duffield JS, Lin SL: Platelet-derived growth factor receptor signaling activates pericyte-myofibroblast transition in obstructive and post-ischemic kidney fibrosis. *Kidney Int* 80: 1170–1181, 2011
24. Ignatz RA, Endo T, Massagué J: Regulation of fibronectin and type I collagen mRNA levels by transforming growth factor-beta. *J Biol Chem* 262: 6443–6446, 1987
25. Yang J, Dai C, Liu Y: Hepatocyte growth factor suppresses renal interstitial myofibroblast activation and intercepts Smad signal transduction. *Am J Pathol* 163: 621–632, 2003
26. Ren S, Johnson BG, Kida Y, Ip C, Davidson KC, Lin SL, Kobayashi A, Lang RA, Hadjantonakis AK, Moon RT, Duffield JS: LRP-6 is a coreceptor for multiple fibrogenic signaling pathways in pericytes and myofibroblasts that are inhibited by DKK-1. *Proc Natl Acad Sci U S A* 110: 1440–1445, 2013
27. Bondi CD, Manickam N, Lee DY, Block K, Gorin Y, Abboud HE, Barnes JL: NAD(P)H oxidase mediates TGF-beta1-induced activation of kidney myofibroblasts. *J Am Soc Nephrol* 21: 93–102, 2010
28. Tennezé L, Daurat V, Tibi A, Chaumet-Riffaud P, Funck-Brentano C: A study of the relative bioavailability of cysteamine hydrochloride, cysteamine bitartrate and phosphocysteamine in healthy adult male volunteers. *Br J Clin Pharmacol* 47: 49–52, 1999
29. Fidler MC, Barshop BA, Gangoiti JA, Deutsch R, Martin M, Schneider JA, Dohil R: Pharmacokinetics of cysteamine bitartrate following gastrointestinal infusion. *Br J Clin Pharmacol* 63: 36–40, 2007
30. Dohil R, Gangoiti JA, Cabrera BL, Fidler M, Schneider JA, Barshop BA: Long-term treatment of cystinosis in children with twice-daily cysteamine. *J Pediatr* 156: 823–827, 2010
31. Gangoiti JA, Fidler M, Cabrera BL, Schneider JA, Barshop BA, Dohil R: Pharmacokinetics of enteric-coated cysteamine bitartrate in healthy adults: A pilot study. *Br J Clin Pharmacol* 70: 376–382, 2010
32. Kawada N, Otogawa K: Role of oxidative stress and Kupffer cells in hepatic fibrosis. *J Gastroenterol Hepatol* 22[Suppl 1]: S85–S86, 2007
33. Kliment CR, Oury TD: Oxidative stress, extracellular matrix targets, and idiopathic pulmonary fibrosis. *Free Radic Biol Med* 49: 707–717, 2010
34. Himmelfarb J, Kane J, McMonagle E, Zaltas E, Bobzin S, Boddupalli S, Phinney S, Miller G: Alpha and gamma tocopherol metabolism in healthy subjects and patients with end-stage renal disease. *Kidney Int* 64: 978–991, 2003
35. Vivekananthan DP, Penn MS, Sapp SK, Hsu A, Topol EJ: Use of antioxidant vitamins for the prevention of cardiovascular disease: Meta-analysis of randomised trials. *Lancet* 361: 2017–2023, 2003
36. Pergola PE, Krauth M, Huff JW, Ferguson DA, Ruiz S, Meyer CJ, Warnock DG: Effect of bardoxolone methyl on kidney function in patients with T2D and stage 3b-4 CKD. *Am J Nephrol* 33: 469–476, 2011
37. Pergola PE, Raskin P, Toto RD, Meyer CJ, Huff JW, Grossman EB, Krauth M, Ruiz S, Audhya P, Christ-Schmidt H, Wittes J, Warnock DG; BEAM Study Investigators: Bardoxolone methyl and kidney function in CKD with type 2 diabetes. *N Engl J Med* 365: 327–336, 2011
38. Hinz B, Phan SH, Thannickal VJ, Prunotto M, Desmoulière A, Varga J, De Wever O, Mareel M, Gabbiani G: Recent developments in myofibroblast biology: Paradigms for connective tissue remodeling. *Am J Pathol* 180: 1340–1355, 2012
39. Humphreys BD, Lin SL, Kobayashi A, Hudson TE, Nowlin BT, Bonventre JV, Valerius MT, McMahon AP, Duffield JS: Fate tracing reveals the pericyte and not epithelial origin of myofibroblasts in kidney fibrosis. *Am J Pathol* 176: 85–97, 2010
40. Lin SL, Kisseleva T, Brenner DA, Duffield JS: Pericytes and perivascular fibroblasts are the primary source of collagen-producing cells in obstructive fibrosis of the kidney. *Am J Pathol* 173: 1617–1627, 2008
41. Schimpf C, Duffield JS: Mechanisms of fibrosis: The role of the pericyte. *Curr Opin Nephrol Hypertens* 20: 297–305, 2011
42. Hecker L, Vittal R, Jones T, Jagirdar R, Luckhardt TR, Horowitz JC, Pennathur S, Martinez FJ, Thannickal VJ: NADPH oxidase-4 mediates myofibroblast activation and fibrogenic responses to lung injury. *Nat Med* 15: 1077–1081, 2009
43. Sampson N, Koziel R, Zenzmaier C, Bubendorf L, Plas E, Jansen-Dürr P, Berger P: ROS signaling by NOX4 drives fibroblast-to-myofibroblast differentiation in the diseased prostatic stroma. *Mol Endocrinol* 25: 503–515, 2011
44. Jézégou A, Llinares E, Anne C, Kieffer-Jaquino S, O'Regan S, Aupetit J, Chabli A, Sagné C, Debacker C, Chadeaux-Vekemans B, Journet A, André B, Gasnier B: Heptahelical protein PQLC2 is a lysosomal cationic amino acid exporter underlying the action of cysteamine in cystinosis therapy. *Proc Natl Acad Sci U S A* 109: E3434–E3443, 2012
45. Go YM, Jones DP: Cysteine/cystine redox signaling in cardiovascular disease. *Free Radic Biol Med* 50: 495–509, 2011
46. Iyer SS, Accardi CJ, Ziegler TR, Blanco RA, Ritzenthaler JD, Rojas M, Roman J, Jones DP: Cysteine redox potential determines pro-inflammatory IL-1beta levels. *PLoS ONE* 4: e5017, 2009
47. Iyer SS, Jones DP, Brigham KL, Rojas M: Oxidation of plasma cysteine/cystine redox state in endotoxin-induced lung injury. *Am J Respir Cell Mol Biol* 40: 90–98, 2009
48. Matsuo S, López-Guisa JM, Cai X, Okamura DM, Alpers CE, Bumgarner RE, Peters MA, Zhang G, Eddy AA: Multifunctionality of PAI-1 in fibrogenesis: Evidence from obstructive nephropathy in PAI-1-overexpressing mice. *Kidney Int* 67: 2221–2238, 2005

This article contains supplemental material online at <http://jasn.asnjournals.org/lookup/suppl/doi:10.1681/ASN.2012090962/-/DCSupplemental>.